Magnetic Resonance in Medicine 69:1634–1644 (2013)

Do Dynamic-Based MR Knee Kinematics Methods Produce the Same Results as Static Methods?

Agnes G. d'Entremont,[1–3]* Jurek A. Nordmeyer-Massner,[4] Clemens Bos,[5] David R. Wilson,[2,3,6] and Klaas P. Pruessmann[4]

MR-based methods provide low risk, noninvasive assessment of joint kinematics; however, these methods often use static positions or require many identical cycles of movement. The study objective was to compare the 3D kinematic results approximated from a series of sequential static poses of the knee with the 3D kinematic results obtained from continuous dynamic movement of the knee. To accomplish this objective, we compared kinematic data from a validated static MR method to a fast static MR method, and compared kinematic data from both static methods to a newly developed dynamic MR method. Ten normal volunteers were imaged using the three kinematic methods (dynamic, static standard, and static fast). Results showed that the two sets of static results were in agreement, indicating that the sequences (standard and fast) may be used interchangeably. Dynamic kinematic results were significantly different from both static results in eight of 11 kinematic parameters: patellar flexion, patellar tilt, patellar proximal translation, patellar lateral translation, patellar anterior translation, tibial abduction, tibial internal rotation, and tibial anterior translation. Three-dimensional MR kinematics measured from dynamic knee motion are often different from those measured in a static knee at several positions, indicating that dynamic-based kinematics provides information that is not obtainable from static scans. **Magn Reson Med 69:1634–1644, 2013. © 2012 Wiley Periodicals, Inc.**

Key words: knee MRI; joint kinematics; dynamic imaging; stretchable coil

In vivo measurement of knee joint kinematics or tracking can be useful in studying disorders at both the patellofemoral and tibiofemoral joints, such as osteoarthritis (1,2), patellofemoral pain (3,4), or anterior cruciate ligament (ACL) injury (5). The primary functions of the knee are to allow movement and transmit load, and a primary aim of surgery is to restore movement and load transmission to normal when these have been disrupted by injury or disease. Load has not been measured directly in vivo in natural joints, but joint movement has. Assessing how joint movement is affected by injury or disease and how effectively it has been corrected, is of substantial interest for improving joint health.

Knee kinematics have been measured in vivo using MR (6–8), CT (9), fluoroscopy, roentgen stereophotogrammetric analysis (RSA), and combinations of these (10,11), optical tracking of markers fixed to bone pins (12), and molded patellar clamps (13). Methods using ionizing radiation and invasive bone pins or fiducial markers have greater potential risks and discomfort for research participants than MR-based methods.

As the knee's primary functions are to move in three dimensions and transmit substantial loads, it makes sense that kinematics should be assessed in three dimensions while the joint is loaded physiologically and moving at a physiological rate, as is done in clinical tests of joint function. However, in most studies of knee kinematics compromises have been made. Two-dimensional (2D) dynamic MR methods (14–16) obtain kinematic information from one slice at a particular flexion angle, which can be problematic because the relationship between 2D measures and 3D kinematics will depend on slice position and orientation, and patient position (17). Differences between static and dynamic 2D measures have been documented for MR and other modalities (9,14,16), but comparisons between 3D static and dynamic MR measures have not been made. 3D dynamic MR knee kinematics methods based on cine-phase contrast (cine-PC) or fast-PC imaging have been developed (18–21). These methods rely on one sagittal image with velocity encoding in three directions, integrated to obtain positions. Subjects are required to repeat the motion as accurately as possible over one or more minutes assisted by an audible beat. Although physiological rates of motion (35 cycles per minute) can be captured with an accuracy that is sufficient to detect clinically relevant changes using these methods, the requirement for careful repetition and large number of cycles required may limit both the loading possibilities and the application in populations with pain or injury. A critical limitation in the context of our research question is that cine-PC methods rely on velocity data for positional information, and velocity is zero in static images. Therefore, cine-PC methods are unable provide direct comparisons between static and dynamic results. Many 3D in vivo assessments of MR kinematics utilize sequential static images acquired over the range of motion (6–8); however, it is unclear how well sequential static postures represent continuous motion of the knee.

The objective of this study was to compare the 3D kinematic results approximated from a series of sequential static poses of the knee with the 3D kinematic results

[1]Department of Mechanical Engineering, University of British Columbia, Canada.
[2]Centre for Hip Health and Mobility, University of British Columbia, Canada.
[3]Vancouver Coastal Health Research Institute, Vancouver, Canada.
[4]Institute for Biomedical Engineering, ETH and University of Zurich, Zurich, Switzerland.
[5]MR Clinical Science, Philips Healthcare, Best, Netherlands.
[6]Department of Orthopaedics, University of British Columbia, Canada.
*Correspondence to: Agnes G. d'Entremont, MASc, Centre for Hip Health and Mobility, Robert H. N. Ho Research Centre, 2635 Laurel Street, Vancouver BC V5Z 1M9, Canada. E-mail: agnesgd@interchange.ubc.ca
Received 9 November 2011; revised 14 June 2012; accepted 27 June 2012.
DOI 10.1002/mrm.24425
Published online 27 July 2012 in Wiley Online Library (wileyonlinelibrary.com).

obtained from continuous dynamic movement of the knee. To accomplish this objective, we compared kinematic data from a validated static MR method to a fast static MR method, and compared kinematic data from both static methods to a newly developed dynamic MR method.

METHODS

We compared 3D knee kinematics measured using a new MR dynamic method to two versions of a sequential static MR method in 10 normal volunteers [seven right and dominant knees, three left and nondominant knees, eight males, ages 28–40 (mean 31), height 179.8 cm (±9.3 cm)]. Volunteers were excluded if they had any MR contraindications, and dominant knees were always scanned unless they had a history of knee injury involving ambulatory aids or knee surgery, in which case the healthy nondominant knee was imaged. All volunteers gave written informed consent, and the study was conducted according to institutional ethics guidelines.

Imaging

All imaging was done on a Philips Achieva 3 T scanner. All knees were imaged using a novel stretchable eight-channel knee coil array which permits knee flexion while maximizing the signal-to-noise ratio independently of the knee size and shape (Fig. 1a) (22). The high-resolution scan of each knee was performed to obtain detailed subject-specific anatomical information (Table 1). To produce loaded flexion, a MR-compatible loading rig was created that allowed free leg motion with a force of 8% body weight applied in the ankle–hip direction (Fig. 1b,c). Foam wedges supported the thigh during scanning. A fast imaging protocol based on a commercially available ultrafast gradient echo sequence with water suppression for increased contrast (Table 1) was developed to image the knee in continuous motion (dynamic). To test whether this sequence produced different kinematic results, it was used to obtain images of static poses (static fast) and compared to the standard sequence (static standard). Three sets of images were taken in loaded flexion: static standard (16 slices, 2D TSE, 23 s), static fast (eight slices, ultrafast gradient echo, 1.9 s), and dynamic (30 sets, eight slices each, ultrafast gradient echo, 56 s; Table 1). The two types of static scans were performed together at each of six flexion angles, for a loaded time at each angle of about 40 s (including a short system delay between scans), after which the weight was removed and the subject was repositioned. Total time taken for all static scans, including positioning, reference scans, and scan planning, was about 30 min. The dynamic scan was performed following six pairs of static scans. Angles for the static scans were chosen to cover the same flexion range as the dynamic scan. The subject was asked to move very slowly during the dynamic scan, but no specific rate of motion was required. Thirty temporal sets of dynamic scans were acquired, each taking 1.9 s, with no interpolation.

Image Processing

Bone models were generated and coordinate systems were defined in them, and they were then registered to the loaded flexion positions from which kinematics were calculated (Fig. 2). All three knee bones were segmented manually from the high-resolution image using Analyze (Mayo Clinic, MN) by one experienced operator to create bone models. Anatomical axes for each bone were defined in the high-resolution models following our established protocol (7,23). Positive patellar rotations were defined as follows: patellar flexion entailed the superior patellar edge rotating anteriorly, patellar tilt

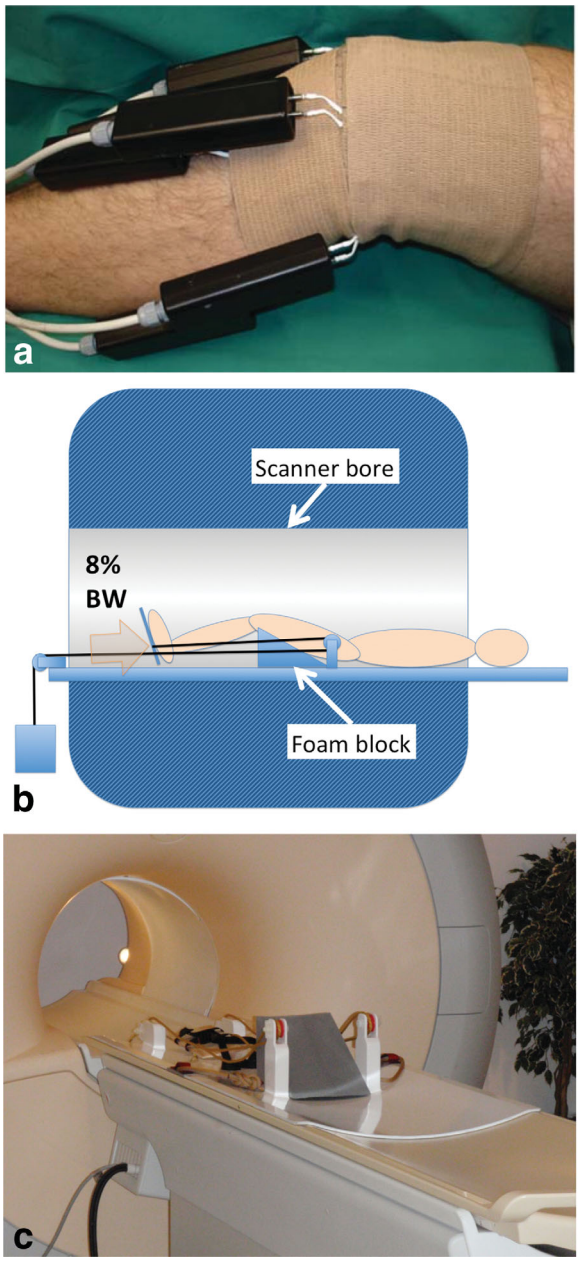

FIG. 1. Stretchable knee coil and loading rig. **a**: Stretchable eight-channel knee coil array (20). **b**: Schematic of loading rig with free floating pedal attached to foot with two straps, and attached with rope on either side of the ankle joint through pulleys to hanging weight. A range of foam wedges were used to support the thigh during static imaging, with the largest of these wedges supporting the thigh as the lower leg was flexed and extended dynamically. **c**: Photo of loading rig on scanner bed. [Color figure can be viewed in the online issue, which is available at wileyonlinelibrary.com.]

Table 1
MRI Sequence Parameters

	High resolution	Static standard	Static fast	Dynamic
Scan type	TSE	TSE	TFE	TFE
Matrix	640 × 640	256 × 256	320 × 320	320 × 320
Slices	46	16	8	8 × 30 sets
Recon voxel (mm)	0.50 × 0.50 × 2	1.25 × 1.25 × 2	1.00 × 1.00 × 5	1.00 × 1.00 × 5
Field of view (mm)	320 × 320	320 × 320	320 × 320	320 × 320
TR (ms)	597	650	2.4	2.4
TE (ms)	15	20	1.20	1.19
Flip angle (°)	90	90	15	15
Slice gap (mm)	0	5	0.5	0.5
Total coverage (mm)	92	107	43.5	43.5
Scan time	8:52	0:23	0:01.9	0:56
TSE/TFE factor	4	8	86	86
Number of averages	2	1	1	1

entailed the medial patellar edge rotating posteriorly, and patellar spin entailed the superior patellar edge rotating medially. Because of the somewhat reduced useable field of view along the leg (a function of the extent of the knee coil), the definition of the long axes of the tibia and femur were altered from the original method (origin to the most superior centroid of the femur shaft or to the most inferior centroid of the tibia shaft) to a direction along the centroids at 25 and 5% from the visible superior end of the femur shaft or the visible inferior end of the tibia shaft. The bone models were then registered to each low-resolution set (static standard, static fast, dynamic) using an iterative closest points algorithm (24). Finally, translations and rotations for the tibia and patella were calculated with respect to the femur (25).

Data Analysis

We assessed whether the new fast sequence, used for static postures, changed the measured kinematics relative to the standard sequence, used for static postures, using the Bland–Altman method for multiple observations per subject (26). The Bland–Altman, or Limits of Agreement (LOA), method is used to compare the results of two different measurement methods to determine if they are sufficiently similar to be able to use one measurement method in place of the other (27). The statistical test used accounted for within-person correlation due to multiple measures at different knee angles per subject. Linear correlations on the LOA plots were performed with standard error estimates allowing for clustering by subject (using a Huber–White sandwich estimator). Assessing the correlation helps to identify if differences between measurement methods change systematically over the range of the value measured.

We assessed whether there was a difference between static standard, static fast and dynamic images. We tested the null hypothesis that there was no difference between the three conditions using a linear mixed-effects model. This statistical test is the most appropriate and accurate for repeated-measures or nested data, particularly with fixed effects (knee angles) that are unequal between subjects (28). The general principle of the method is to apply individual regression models to each subject and condition, then compare between conditions (within person comparison). The general model was:

$$y_{ij} = \beta_{0j} + \beta_{1j} * \text{knee\_angle} + \beta_2 * \text{knee\_angle}^2 + \beta_3 * \text{condition}_i + \beta_4 * \text{knee\_angle} * \text{condition}_i + \beta_5 * \text{knee\_angle}^2 * \text{condition}_i \quad [1]$$

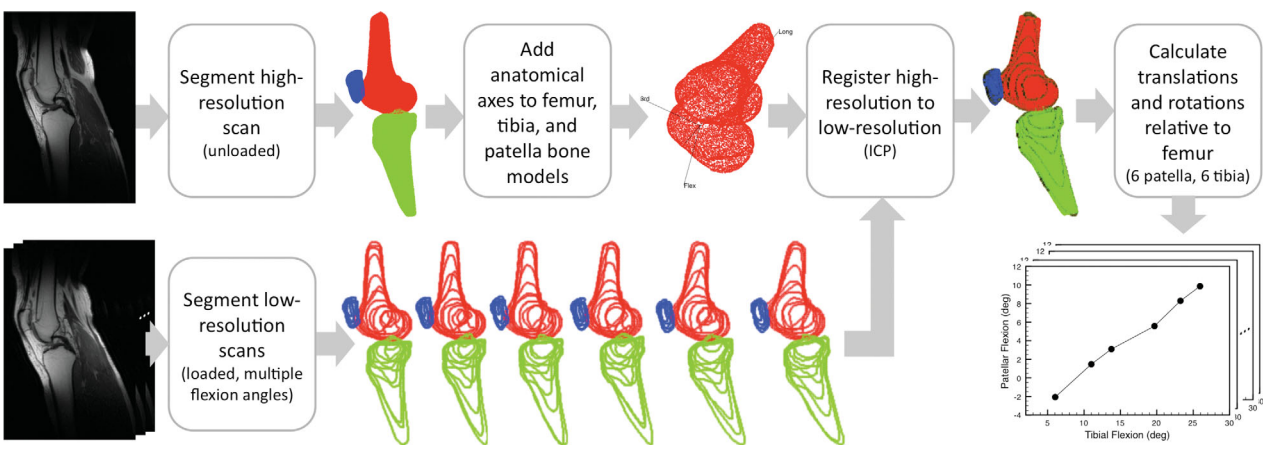

FIG. 2. Flowchart of image processing procedure for obtaining kinematic data. Example showing six static standard flexion angles for one subject.

where y is any one of the 11 kinematic parameters, j = 1–10 (individuals) and i = 1, 2, 3 (conditions). Knee angles were obtained from 3D models. Condition 1 was dynamic (coefficients β_0, β_1, β_2), condition 2 was static fast (add β_3, β_4, β_5 for condition 2), and condition 3 was static standard (add β_3, β_4, β_5 for condition 3). Individuals (j) were allowed to vary in both intercept and slope from the mean:

$$\beta_{0j} = \gamma_0 + u_{0j} \quad [2]$$

$$\beta_{1j} = \gamma_1 + u_{1j} \quad [3]$$

where Eq. 2 represents intercept and Eq. 3 represents slope; γ is the mean value for all subjects, and u is the value for individual subjects.

The quadratic terms (β_2, β_5), u_{1j} (part of β_1) and knee_angle*condition (β_4) were included when they improved the model (as compared to the linear model) as determined by lowering the Bayesian information criterion, which indicates quality of fit but penalizes for extra terms in the model. Statistical analyses were performed using Stata 10.1 (StataCorp, TX).

Observations were made from comparisons of the varying position of the slice stack and direction of motion, but since these were not the designed outcomes of the study statistical analysis was not performed. We observed the effect of slice stack position within the knee on the kinematic results. Static fast images with 16 slices (87.3 mm coverage) were obtained in a relaxed position for four subjects (seven through 10). The images were segmented and then nine subsets of eight slices each were used to compare to the kinematic results from the full 16-slice set.

Repeated dynamic cycles with turnaround points removed were used to calculate intraclass correlation (ICC) results (from linear mixed-effects models) as an estimate of repeatability.

RESULTS

Subjects performed between two and four dynamic flexion–extension cycles {mean 2.75 (standard deviation [SD] 0.7) cycles} in the 56 s scan time, for an average rate of motion of 0.9 (SD 0.2) degrees/s (range 0.6–1 degrees/s). Tibial flexion for all subjects ranged between a mean lowest flexion angle of 8.1 (SD 2.5) and mean highest flexion angle of 29.1° (SD 3.5; overall range 4.2–36.4°). Sample images are presented in Fig. 3.

Bland–Altman analysis, evaluating the agreement between the static fast and static standard sequences, resulted in overall mean differences of 0.15° and 0.36 mm (Table 2), and average ranges of LOA of ±2.07° or ±1.09 mm. Through-plane translations showed the largest ranges of LOA for translations (patellar lateral translation at ±1.4 mm, and tibial lateral translation at ±1.7 mm). Rotations out of the plane (patellar spin, patellar tilt, tibial abduction, and tibial internal rotation) had the largest ranges of LOA and three out of four had the lowest p values in the linear regression. Significant correlations (trends) between differences in each kinematic measure and mean measure were found for patellar tilt and tibial abduction (Fig. 4). Linear regression on the Bland–Altman plots showed a change in difference between the two static methods of 1.3° for every 10° of abduction and 0.25° for every 10° of patellar tilt over the range measured. The LOA obtained using correct standard error estimates for multiple comparisons were a mean 1.9% (SD 0.7%) larger in range than those obtained by assuming independent observations.

Our findings indicate that 3D dynamic kinematic results are different from static results. We found significant kinematic differences between dynamic imaging and both types of static imaging (static fast and static standard) for eight out of 11 kinematic parameters: patellar flexion, patellar tilt, patellar proximal translation, patellar lateral translation, patellar anterior translation, tibial abduction, tibial internal rotation, and tibial anterior translation (Table 3 and Fig. 5). All of the included slope and quadratic terms show differences between dynamic and both static results, and no differences between the static results. Tibial proximal translation and tibial lateral translation showed differences in intercept between static fast and static standard. For tibial proximal translation, there was no statistical difference between dynamic and static fast in intercept, but there were differences for slope.

At full extension, mean absolute differences between the dynamic and static models with statistically different intercepts were 2.0 mm and 2.9°, and near the other end of the range (35°) the mean absolute differences between these same models were 1.9 mm and 3.6°. Difference values for patellar flexion, patellar proximal translation, patellar anterior translation, tibial internal rotation, and tibial anterior translation were outside of the LOA (upper LOA minus lower LOA, Table 2), indicating that they are not likely due to differences between the standard and fast sequences. Difference values for tibial abduction and patellar tilt were not outside the LOA, likely due to the trends leading to larger LOA. Together with the Bland–Altman results, these findings indicate that 3D dynamic kinematic results are different from static results.

Kinematic parameter values were affected by the position of the stack and the number of slices capturing a particular bone (Fig. 6). Typically, stacks that were positioned centrally had values close to the full stack, and those with more slices containing a particular bone also had values closer to the full stack values. For the low-resolution scans, the number of slices containing a particular bone varied between subjects (due to subject size), and within subjects (due to subject position and orientation, and slice stack position).

ICC values for repeated dynamic cycles ranged from 0.840 (95% CI: 0.711, 0.969) for patellar spin, to 0.991 (95% CI: 0.984, 0.999) for patellar anterior translation.

DISCUSSION

In this article, we directly compared knee kinematic results from a dynamic 3D method in MR to kinematics obtained from a series of static poses. We found that the dynamic results are, in most cases, different from both static standard and static fast. In addition to the expected axial plane differences in patellar lateral translation and patellar tilt from the literature, differences

FIG. 3. Sample images from the stretchable knee coil for one subject. High-resolution, and the three types of low-resolution scans (static standard, static fast, and the first 12 of 30 dynamic scans, representing a full motion cycle). The bone edges are discernable on even the low-resolution dynamic images.

between static and dynamic results were seen in kinematic parameters in all planes and both joints. The finding that there are differences between 3D kinematics for static and dynamic conditions is important because it suggests that static imaging does not provide a complete reflection of joint position and orientation during physiologic activity. Differences in pathological joints may be larger.

Range of motion is limited by scanner bore size and subject limb segment length (related to subject height). The range of motion obtained in this study is similar to that of Seisler and Sheehan (35° attained by 30% or more of subjects) and Barrance et al. (25°), who had smaller mean subject heights (172.3 and 178 cm, respectively, compared to 179.8 cm in this study) (20,29). The range of motion was not limited by the stretchable coil.

The Bland–Altman analysis indicates that differences between static and dynamic results are likely not due to the new fast sequence, but are instead due to differences in motion. Previous work indicates that the biases and LOA found in our study show agreement between the static fast and static standard methods. Intrasubject variability (repeatability, grand mean error) using a static standard scan (as measured in vivo for the patellofemoral joint) was found to be 0.30–1.75° and 0.47 to 0.88 mm, depending on the parameter (7), which is larger than the mean biases seen here. Significant differences in patellar flexion (7.5°), patellar spin (6.4°), patellar proximal

Table 2
Bland–Altman Results

	Limits of agreement			Linear regression (trend)		
	Upper LOA	Mean diff.	Lower LOA	Coefficient	SE	*P*-value
Patellar flexion (°)	1.96	0.44	−1.08	0.01	0.01	0.592
Patellar spin (°)	3.65	0.11	−3.43	−0.06	0.09	0.519
Patellar tilt (°)	2.45	−0.08	−2.60	**−0.03**	**0.01**	**0.017**
Patellar proximal translation (mm)	0.65	−0.50	−1.65	−0.01	0.02	0.538
Patellar lateral translation (mm)	1.54	0.17	−1.21	0.05	0.05	0.346
Patellar anterior translation (mm)	0.74	0.18	−0.39	−0.02	0.02	0.412
Tibial flexion (°)	1.01	0.18	−0.64	0.01	0.01	0.379
Tibial abduction (°)	2.05	0.01	−2.02	**−0.13**	**0.04**	**0.017**
Tibial internal rotation (°)	2.04	0.06	−1.92	0.05	0.03	0.098
Tibial proximal translation (mm)	0.42	−0.45	−1.32	0.01	0.05	0.797
Tibial lateral translation (mm)	1.11	−0.61	−2.33	0.07	0.07	0.339
Tibial anterior translation (mm)	0.58	−0.28	−1.13	0.00	0.03	0.865

Limits of agreement (LOA) show the upper and lower limits of agreement and the mean difference (bias) in mm or degrees, depending on the parameter. Linear regression shows trend results, with coefficient and standard error in mm or degrees, depending on the parameter, and *P*-value. Bold values highlight linear regressions with statistically significant trends.

translation (8.8 mm), and patellar anterior translation (6.6 mm) using the static standard method have been seen between populations with varus and valgus malalignments and knee osteoarthritis (1)—with the exception of patellar spin, the values are outside the LOA in this study (upper LOA minus lower LOA). Differences in anterior translation between knees in ACL-injured noncopers has been found to be 2.6–3 mm depending on knee angle (29), which is outside the LOA in this study. Together these results suggest that differences seen with actual motion are likely not related to the fast sequence, and that clinically relevant differences may be detected. Out of plane rotations may be most affected by the more limited coverage in the medial–lateral direction in the static fast scans, resulting in larger LOA and trends (patellar tilt and tibial abduction). In normal subjects, tibial abduction for activities of daily living ranges within −2.2 to 10.0° (30), and patellar tilt ranges from 12.5 to 19.2° in supine extension from 40° (20). Therefore with the trends observed, the largest differences between the two static methods over a range of motion in normal activities are 1.1° for tibial abduction and 0.3° for patellar tilt, which are still in the range of the grand mean error of the original method.

Our findings that 3D dynamic kinematic results are different from static results are consistent (pattern of change) with those seen in 2D measures of patellar lateral displacement and patellar tilt angle in both MR (14,16) and CT (9) (Fig. 7). Actual values of 3D dynamic kinematic parameters (both patellar and tibial) are consistent in range and pattern with those measured in normals with a cine-PC/fast-PC method by Seisler and Sheehan (20) except for tibial proximal translation (pattern, range) and tibial anterior translation (range) (Table 4). These differences in tibial translations may be attributed to differences in the tibial origin location (tibial tubercule rather than the most superior point of the tibial spines in the current study). Barrance et al., using

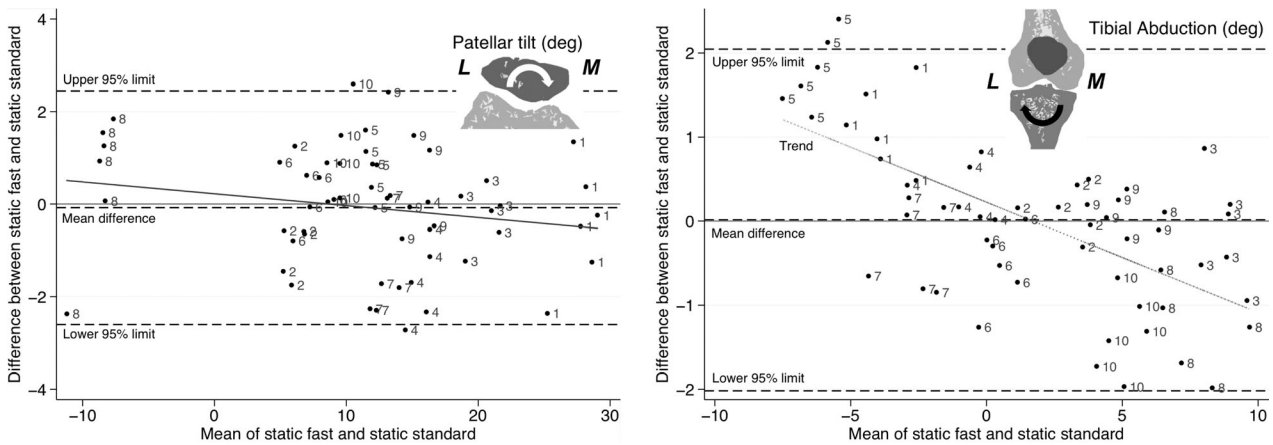

FIG. 4. Bland–Altman plots of **a:** patellar tilt and **b:** tibial abduction. For each subject and flexion angle, the difference between static fast and static standard results has been plotted against the mean of static fast and static standard results. Individual points labeled with subject number (1–10), six points per subject. LOA show the upper and lower LOA (95% of points lie within) and the mean difference (bias) in degrees. Trend lines plotted for each parameter. These two parameters were the only ones to have statistically significant trends in difference versus mean.

Table 3
Mixed Linear Model Results

				β_3 (difference in intercept)		
	β_0 (intercept)	β_1 (knee_angle)	β_2 (knee_angle^2)	DYN to SF	DYN to SS	SF to SS
Patellar flexion (°)	−7.63 (1.07)***	0.51 (0.02)***	Not included	**−1.64 (0.50)*****	**−1.95 (0.50)*****	0.31 (0.61)
Patellar spin (°)	−4.22 (1.22)***	0.05 (0.02)**	Not included	−0.11 (0.28)	−0.21 (0.28)	0.10 (0.36)
Patellar tilt (°)	6.85 (3.37)*	0.42 (0.08)***	−0.008 (0.002)***	**4.08 (0.59)*****	**4.14 (0.59)*****	−0.06 (0.71)
Patellar proximal translation (mm)	39.82 (1.87)***	−0.80 (0.06)***	0.000 (0.002)	**−2.79 (0.89)****	**−2.25 (0.90)****	−0.53 (1.01)
Patellar lateral translation (mm)	−0.78 (1.14)	−0.07 (0.03)*	Not included	**−3.42 (0.41)*****	**−3.72 (0.41)*****	0.30 (0.51)
Patellar anterior translation (mm)	26.47 (1.10)***	0.27 (0.03)***	−0.007 (0.001)***	**−0.62 (0.32)***	**−0.93 (0.32)****	0.31 (0.36)
Tibial abduction (°)	−1.31 (1.33)	0.09 (0.01)***	Not included	**1.24 (0.12)*****	**1.24 (0.12)*****	0.00 (0.15)
Tibial internal rotation (°)	−1.98 (2.01)	0.56 (0.13)***	−0.010 (0.003)**	**4.31 (2.11)***	**4.66 (2.14)***	−0.36 (2.54)
Tibial proximal translation (mm)	−7.27 (0.62)***	0.01 (0.02)	0.002 (0.000)***	−0.22 (0.16)	**0.40 (0.16)***	**−0.62 (0.20)****
Tibial lateral translation (mm)	−4.33 (0.36)***	−0.09 (0.01)***	Not included	**−1.17 (0.10)*****	**−0.58 (0.10)*****	**−0.60 (0.13)*****
Tibial anterior translation (mm)	−14.35 (0.72)***	−0.39 (0.05)***	0.004 (0.001)***	**−1.16 (0.37)****	**−0.97 (0.37)****	−0.19 (0.46)

	β_4 (difference in knee_angle)			β_5 (difference in knee_angle^2)		
	DYN to SF	DYN to SS	SF to SS	DYN to SF	DYN to SS	SF to SS
Patellar flexion (°)	**0.20 (0.02)*****	**0.20 (0.02)*****	0.00 (0.03)	Not included in model		
Patellar spin (°)	Not included in model			Not included in model		
Patellar tilt (°)	**−0.21 (0.03)*****	**−0.21 (0.03)*****	0.00 (0.03)	Not included in model		
Patellar proximal translation (mm)	**−0.25 (0.10)****	**−0.27 (0.10)****	0.01 (0.11)	**0.008 (0.002)*****	**0.009 (0.003)*****	0.000 (0.003)
Patellar lateral translation (mm)	**0.14 (0.02)*****	**0.15 (0.02)*****	−0.01 (0.02)	Not included in model		
Patellar anterior translation (mm)	**0.14 (0.03)*****	**0.15 (0.04)*****	−0.01 (0.04)	**−0.004 (0.001)*****	**−0.005 (0.001)*****	0.000 (0.001)
Tibial abduction (°)	Not included in model			Not included in model		
Tibial internal rotation (°)	**−1.04 (0.23)*****	**−1.12 (0.24)*****	0.07 (0.28)	**0.022 (0.006)*****	**0.025 (0.006)*****	−0.002 (0.007)
Tibial proximal translation (mm)	**0.04 (0.01)*****	**0.03 (0.01)*****	0.01 (0.01)	Not included in model		
Tibial lateral translation (mm)	Not included in model			Not included in model		
Tibial anterior translation (mm)	**−0.07 (0.02)*****	**−0.07 (0.02)*****	0.00 (0.02)	Not included in model		

β_0 is the constant term, β_1 is the linear term, and β_2 is the quadratic term (if included in model) for the dynamic results. β_3 is the difference in the constant term between two conditions (DYN = dynamic, SS = static standard, SF = static fast). β_4 is the difference in the linear term between two conditions (if condition by linear term was included in model), and β_5 is the difference in the quadratic term between two conditions (if condition by quadratic term was included in model). The term u_{1j} (individual slope, Eq. 3) was included in the model for all parameters except patellar spin and tibial internal rotation. Mean and standard deviation of model values; units of mm or deg depending on parameter; *P =< 0.05, **P =< 0.01, ***P =< 0.001. Bold values highlight statistically significant model parameters that show differences between conditions.

another cine-PC method, show similar results to our dynamic results in control subjects for tibial anterior translation and tibial internal rotation, the only parameters reported (29) (Table 4). Actual values of 3D static PF kinematic parameters are similar to those measured by Fellows et al. (23), and the normal subjects from MacIntyre et al. (4) (with only patellar lateral translation having a different pattern) (Table 4). Patel and colleagues normalized for size in their 3D PF kinematic data; patellar spin was consistent, and patellar tilt (pattern and range) and patellar proximal translation (pattern) were slightly different (31). Patel et al. (6) normalized for size and shifted full extension values to 0 mm or degrees in their 3D TF kinematic data; patterns and ranges for parameters are consistent for tibial anterial translation, tibial abduction, and tibial lateral translation, whereas the pattern of tibial internal rotation was slightly different (Table 4). It is known that the range of normal values in patellar kinematics is wide (32). The range of values of tibial kinematics is also wide in this study, for example, tibial internal rotation has an average range of values of 25.6° over the three types of low-resolution scans (23.2–29.3°). This is consistent with Seisler and Sheehan, where ±2 SD at a representative flexion angle containing data from all subjects gives a range of 25.6° (20). Some of the differences noted may be related to the range of motion available in this study, and the consequent model shape fit to the data (e.g., linear model fits

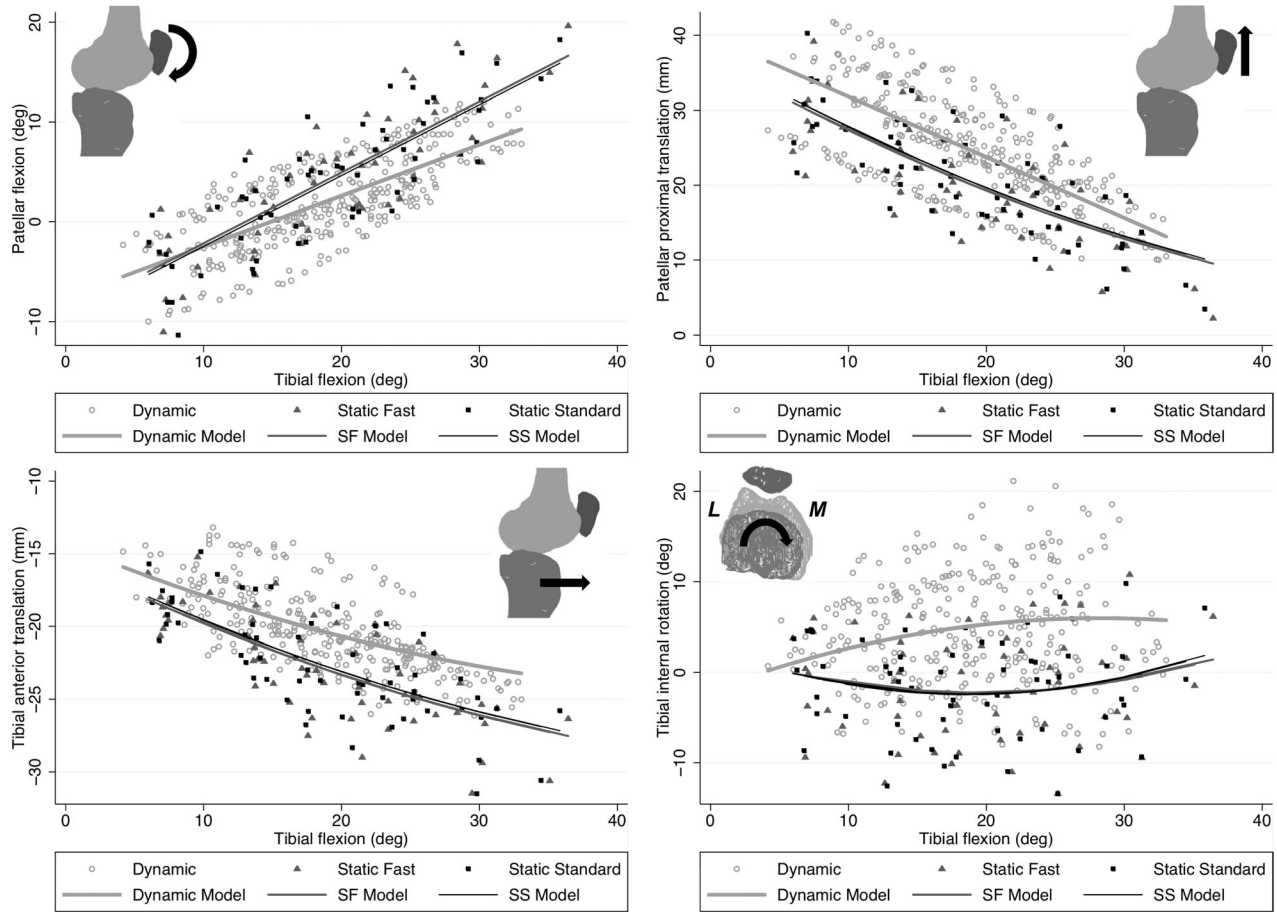

FIG. 5. Selected kinematics results, with data points for 10 subjects and mixed-effects models chosen based on lowest Bayesian information criterion for three type of low resolution scans. **a**: Patellar flexion, **b:** patellar proximal translation, **c:** tibial anterior translation, **d:** tibial internal rotation, all plotted version tibial flexion (knee flexion angle). (DYN = dynamic, SF = static fast, SS = static standard).

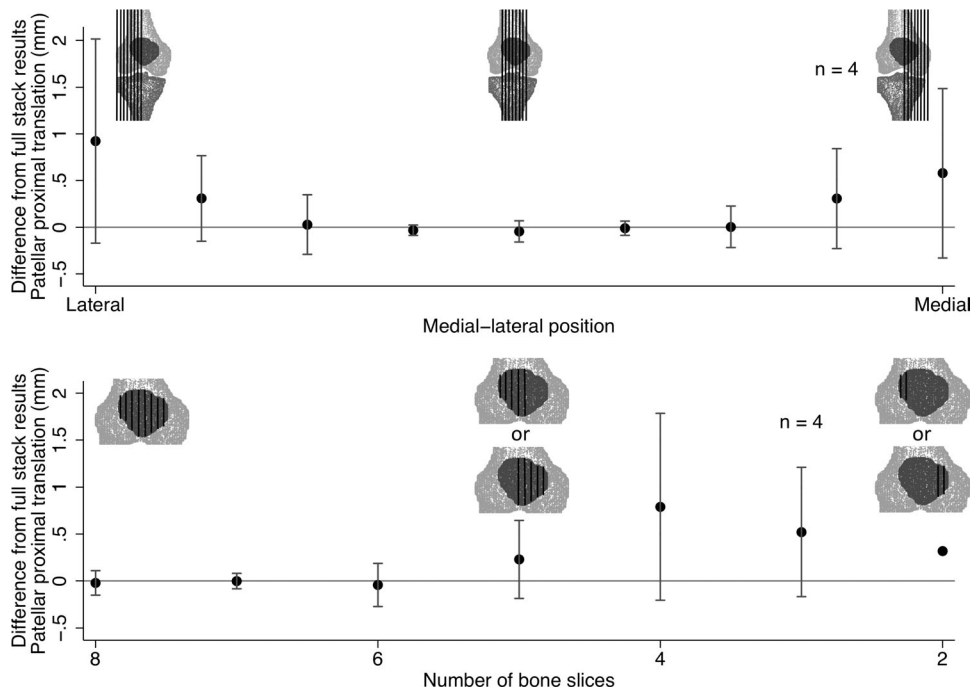

FIG. 6. Typical result from slice stack analysis. Patellar proximal translation, difference between subset and full 16-slice stack result (mean and SD for four subjects), plotted **a:** versus medial–lateral position (average and SD of parameter difference) and **b:** versus number of slices containing patella. Diagrams indicate generalized slice locations for various medial–lateral positions and bone slice numbers.

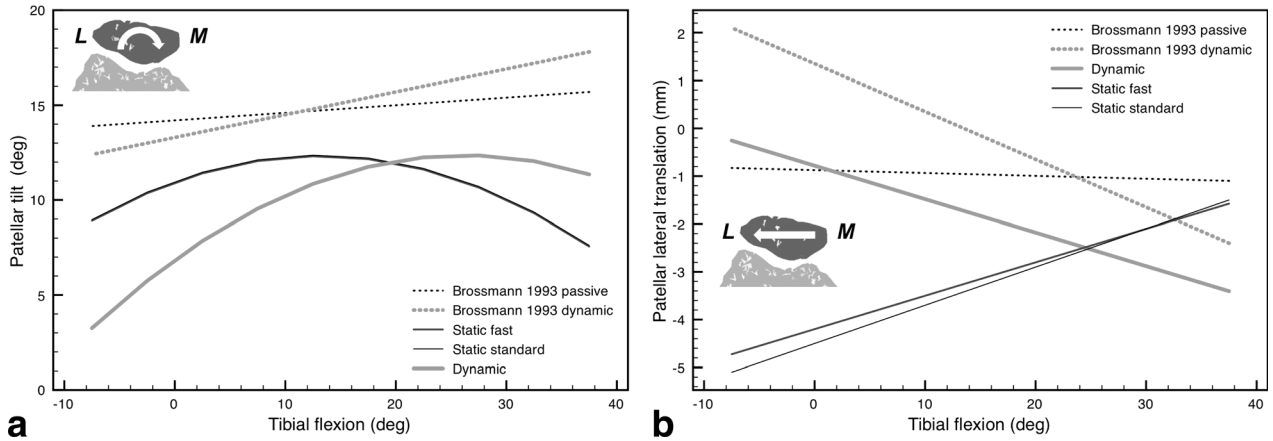

FIG. 7. Comparison plot between 2D passive (static) and dynamic MR results from Brossmann et al. (16), and 3D static and dynamic results from the current study for **a:** patellar tilt and **b:** patellar lateral translation.

slightly quadratic data well over some ranges). There are also differences in types and magnitudes of loading between studies, which may affect results (33). Differences in results may also be attributed to differences in the definition of bone coordinate systems, as mentioned above, which are known to affect results (34).

It is not surprising that, compared to the results from 16 slices of static fast, eight slice sub-sets of static fast images showed varying values of kinematic parameters depending on number of slices capturing bone (especially for patella) and position of slice stack in medial–lateral direction (e.g., centered or off centre). The ideal position of the slice stack has been shown to be centered medial–lateral on the knee, especially covering the patella completely. It is likely that the central position provides information from the tibial and femoral shafts, which more accurately orients those bones in space, and the patella, having fewer distinct landmarks, produces a better result when a maximum of information is provided.

Although the estimate of repeatability (ICC) calculated using repeated dynamic cycles for each subject is not an overall measure of repeatability for the method, it does indicate that the procedure from imaging to data analysis has sufficient repeatability to address clinically relevant research questions. Patellar spin had the lowest ICC at 0.840, and is often found to be quite variable (32). All other ICCs were at or above 0.925.

Table 4
Ranges of Parameter Values: Comparison to Published Values from 3D MR Kinematics Studies (Static and Dynamic)

	Static						Dynamic		
Tibial flexion range	Current study (SS) $n = 10$ 10°–35°	MacIntyre et al. (4) (controls) $n = 20$ 10°–35°	Patel et al. (6) $n = 10$ 10°–35°	Patel et al. (31) $n = 10$ 10°–35°	Current study (SS) $n = 10$ 5°–30°	Fellows et al. (23) $n = 1$ 5°–30°	Current study (DYN) $n = 10$ 5°–30°	Seisler and Sheehan (20) $n = 22$ (5°) or 23 (30°)	Barrance et al. (29) (controls) $n = 10$ 5°–30°
Patellar flexion (°)	**17.8**	14.9			**17.8**	15	**12.8**	13.5	
Patellar spin (°)	**1.3**	1.5		1.9	**1.3**	5	**1.3**	0.0	
Patellar tilt (°)	**−3.8**	2.5		0.8	**−1.8**	−3	**3.5**	4.1	
Patellar proximal translation (mm)	**−16.6**	−16.9		−11.0	**−18.9**	−12	**−20.0**	−16.7	
Patellar lateral translation (mm)	**2.0**	−1.6			**2.0**	2	**−1.8**	−2.8	
Patellar anterior translation (mm)	**−3.0**	−0.7			**0.0**	−4	**0.6**	2.4	
Tibial abduction (°)	**2.3**		3.2				**2.3**	−1.6	
Tibial internal rotation (°)	**2.9**		2.7				**5.3**	4.4	5.0
Tibial proximal translation (mm)	**3.3**						**2.0**	−9.2	
Tibial lateral translation (mm)	**−2.3**		−1.0				**−2.3**	−5.1	
Tibial anterior translation (mm)	**−7.0**		−8.0				**−6.3**	−19.6	−5.0

Selected 15° ranges of tibial flexion were compared based on range available in current study and range available in study from literature. All reported parameters included (DYN = dynamic, SS = static standard).

Strengths of the method include allowing subjects to use a self-selected rate of motion, collecting all data in two to four cycles, and obtaining more data points in a shorter time than static methods which all may reduce subject burden. We could alternately have subjects move at a specific rate by providing audible or visual feedback. It is possible to apply the same methodology using cine images in place of ultrafast gradient echo images and obtain higher rates of motions (similar scan time, similar flexion, angle number). We may be able to apply loads closer to those seen in activities of daily living, due to the short scan time. Studies comparing load magnitudes and types have found significant differences in several kinematic parameters with changes in loading (3,33). Strengths of this study include making a direct comparison to validated static method, studying a clinically important range of motion [for example, patellar subluxation is associated with lateral translation of the patella in the first 20° of knee flexion (35)], and loading the joint, which provides a mechanical environment closer to that of daily activities.

A limitation of this study was that static positions differ from dynamic positions (different hip flexion at same knee flexion angles), due to the technical and practical requirements of static and dynamic scanning. There were several indications that the effect of this difference may be small. For one subject, there was little observable difference between the static and dynamic scans. For all subjects, the most flexed position in both static and dynamic is the same position; however these did not typically produce the same values. 2D studies have seen similar differences between static and dynamic kinematics. Together this indicates that the differences seen between static and dynamic results are likely due to movement. Although we do not have a direct assessment of accuracy, larger or smaller standard error (noise) in the dynamic results is unlikely to influence the overall conclusions of the study, which is that dynamic and static kinematic results are different. Although we were able to apply an axial load to the leg during imaging, the load magnitude was much smaller than that expected in activities of daily living. A limitation of this method was that we are currently restricted to slow motion [20 s/cycle compared to 1.7 s/cycle for cine-PC/fast-PC (20)]; however, we saw similar differences between static and dynamic measures as those from Brossmann et al. with about 1.3 s/cycle (16). It is likely that moving into a position under load requires different muscle activation than being placed in position and subsequently loaded, which results in different kinematics. Our subjects moved at self-selected rates of motion, which introduces potential variability. The similarity with Brossmann's work at higher rate of motion seems to indicate that the differences between rates of motion would not affect the overall conclusions of the study.

A further limitation of the study is that the stretchable knee coil may alter patellar kinematics. As it is not designed to medialize the patella (as in many knee sleeves and braces), and our subjects did not have any diagnosed PF disorders, the effect may be different from the changes reported in the literature, namely the patella being more medial, more posterior, and having more positive medial tilt with a brace (36–41).

Although we have assessed the agreement of the new sequence with measurements from a validated method, rather than a direct assessment of accuracy, the size of the LOA and the magnitudes of clinically important differences in the literature imply that the static fast/dynamic method may be able to detect relevant kinematic differences between populations. McWalter et al. found significant differences in patellar flexion, patellar proximal translation, and patellar anterior translation between populations with varus and valgus malalignments and knee osteoarthritis using the static standard method that are outside the LOA in this study (1). Barrance et al. found significant side-to-side differences in tibial anterior position in ACL-injured non-copers with uninjured contralateral knees that are also outside the LOA in this study (29). Although it has been shown that kinematic measures from a series of static positions can distinguish kinematic features between groups, dynamic scanning has the capability of eliciting distinct information about joint function. The short scan time and few knee cycles required may be beneficial for increasing the load applied to the joint to better represent the typical mechanical environment, reducing the burden on populations with pain or other movement difficulties, and reducing imaging cost.

Further work comparing static and dynamic imaging in joints with documented abnormalities, such as ACL-deficiency or patellofemoral dysmorphism, would be of interest, as the relative differences between the static and dynamic results may vary compared to the healthy normals in this study.

In this study, we have demonstrated the utility of a novel stretchable knee coil for fast imaging of a moving knee, providing images that are acceptable for use in kinematic analysis in a short time, and comfortably allowing flexion. We have shown that a new fast scan provides results that agree with the standard scans for our knee kinematics method, indicating that we can interchangeably use the fast scan for measuring kinematics. We found that 3D MR kinematics measured from dynamic knee motion are often different from those measured in a static knee at several positions, indicating that dynamic kinematics provides information that is not obtainable from static scans.

REFERENCES

1. McWalter EJ, Cibere J, MacIntyre NJ, Nicolaou S, Schulzer M, Wilson DR. Relationship between varus-valgus alignment and patellar kinematics in individuals with knee osteoarthritis. J Bone Joint Surg Am 2007;89:2723–2731.
2. Hinterwimmer S, von Eisenhart-Rothe R, Siebert M, Welsch F, Vogl T, Graichen H. Patella kinematics and patello-femoral contact areas in patients with genu varum and mild osteoarthritis. Clin Biomech (Bristol, Avon) 2004;19:704–710.
3. Draper CE, Besier TF, Fredericson M, Santos JM, Beaupre GS, Delp SL, Gold GE. Differences in patellofemoral kinematics between weight-bearing and non-weight-bearing conditions in patients with patellofemoral pain. J Orthop Res 2011;29:312–317.
4. MacIntyre NJ, Hill NA, Fellows RA, Ellis RE, Wilson DR. Patellofemoral joint kinematics in individuals with and without patellofemoral pain syndrome. J Bone Joint Surg Am 2006;88:2596–2605.
5. Carpenter RD, Majumdar S, Ma CB. Magnetic resonance imaging of 3-dimensional in vivo tibiofemoral kinematics in anterior cruciate ligament-reconstructed knees. Arthroscopy 2009;25:760–766.

6. Patel VV, Hall K, Ries M, Lotz J, Ozhinsky E, Lindsey C, Lu Y, Majumdar S. A three-dimensional MRI analysis of knee kinematics. J Orthop Res 2004;22:283–292.
7. Fellows RA, Hill NA, Gill HS, MacIntyre NJ, Harrison MM, Ellis RE, Wilson DR. Magnetic resonance imaging for in vivo assessment of three-dimensional patellar tracking. J Biomech 2005;38:1643–1652.
8. von Eisenhart-Rothe R, Siebert M, Bringmann C, Vogl T, Englmeier KH, Graichen H. A new in vivo technique for determination of 3D kinematics and contact areas of the patello-femoral and tibio-femoral joint. J Biomech 2004;37:927–934.
9. Dupuy DE, Hangen DH, Zachazewski JE, Boland AL, Palmer W. Kinematic CT of the patellofemoral joint. AJR Am J Roentgenol 1997; 169:211–215.
10. Anderst WJ, Tashman S. The association between velocity of the center of closest proximity on subchondral bones and osteoarthritis progression. J Orthop Res 2009;27:71–77.
11. Fregly BJ, Rahman HA, Banks SA. Theoretical accuracy of model-based shape matching for measuring natural knee kinematics with single-plane fluoroscopy. J Biomech Eng 2005;127:692–699.
12. Koh TJ, Grabiner MD, De Swart RJ. In vivo tracking of the human patella. J Biomech 1992;25:637–643.
13. Wilson NA, Press JM, Koh JL, Hendrix RW, Zhang L-Q. In vivo noninvasive evaluation of abnormal patellar tracking during squatting in patients with patellofemoral pain. J Bone Joint Surg Am 2009;91: 558–566.
14. Muhle C, Brossmann J, Melchert UH, Schroder C, de Boer R, Spielmann RP, Heller M. Functional MRI of the femoropatellar joint: comparison of ultrafast MRI, motion-triggered cine MRI and static MRI. Eur Radiol 1995;5:371–378.
15. Draper CE, Santos JM, Kourtis LC, Besier TF, Fredericson M, Beaupre GS, Gold GE, Delp SL. Feasibility of using real-time MRI to measure joint kinematics in 1.5T and open-bore 0.5T systems. J Magn Reson Imaging 2008;28:158–166.
16. Brossmann J, Muhle C, Schroder C, Melchert UH, Bull CC, Spielmann RP, Heller M. Patellar tracking patterns during active and passive knee extension: evaluation with motion-triggered cine MR imaging. Radiology 1993;187:205–212.
17. Shibanuma N, Sheehan FT, Stanhope SJ. Limb positioning is critical for defining patellofemoral alignment and femoral shape. Clin Orthop Relat Res 2005;434:198–206.
18. Barrance PJ, Williams GN, Novotny JE, Buchanan TS. A Method for measurement of joint kinematics in vivo by registration of 3-D geometric models with cine phase contrast magnetic resonance imaging data. J Biomech Eng 2005;127:829–837.
19. Sheehan FT, Zajac FE, Drace JE. In vivo tracking of the human patella using cine phase contrast magnetic resonance imaging. J Biomech Eng 1999;121:650–656.
20. Seisler AR, Sheehan FT. Normative three-dimensional patellofemoral and tibiofemoral kinematics: a dynamic, in vivo study. IEEE Trans Biomed Eng 2007;54:1333–1341.
21. Behnam AJ, Herzka DA, Sheehan FT. Assessing the accuracy and precision of musculoskeletal motion tracking using cine-PC MRI on a 3.0T platform. J Biomech 2011;44:193–197.
22. Nordmeyer-Massner JA, De Zanche N, Pruessmann KP. Stretchable coil arrays: application to knee imaging under varying flexion angles. Magn Reson Med 2012;67:872–879.
23. Fellows RA, Hill NA, Macintyre NJ, Harrison MM, Ellis RE, Wilson DR. Repeatability of a novel technique for in vivo measurement of three-dimensional patellar tracking using magnetic resonance imaging. J Magn Reson Imaging 2005;22:145–153.
24. Besl PJ, McKay ND. A method for registration of 3-D shapes. IEEE Trans Pattern Anal Mach Intell 1992;14:239–256.
25. Cole GK, Nigg BM, Ronsky JL, Yeadon MR. Application of the joint coordinate system to three-dimensional joint attitude and movement representation: a standardization proposal. J Biomech Eng 1993;115:344–349.
26. Bland JM, Altman DG. Agreement between methods of measurement with multiple observations per individual. J Biopharm Stat 2007;17: 571–582.
27. Bland JM, Altman DG. Statistical methods for assessing agreement between two methods of clinical measurement. Lancet 1986;327: 307–310.
28. Blackwell E, de Leon CFM, Miller GE. Applying mixed regression models to the analysis of repeated-measures data in psychosomatic medicine. Psychosom Med 2006;68:870–878.
29. Barrance PJ, Williams GN, Snyder-Mackler L, Buchanan TS. Do ACL-injured copers exhibit differences in knee kinematics? An MRI study. Clin Orthop Relat Res 2007;454:74–80.
30. Desloovere K, Wong P, Swings L, Callewaert B, Vandenneucker H, Leardini A. Range of motion and repeatability of knee kinematics for 11 clinically relevant motor tasks. Gait Posture 2010;32:597–602.
31. Patel VV, Hall K, Ries M, Lindsey C, Ozhinsky E, Lu Y, Majumdar S. Magnetic resonance imaging of patellofemoral kinematics with weight-bearing. J Bone Joint Surg Am 2003;85-A:2419–2424.
32. Katchburian MV, Bull AMJ, Shih Y-F, Heatley FW, Amis AA. Measurement of patellar tracking: assessment and analysis of the literature. Clin Orthop Relat Res 2003;412:241–259.
33. McWalter EJ, Hunter DJ, Wilson DR. The effect of load magnitude on three-dimensional patellar kinematics in vivo. J Biomech 2010;43: 1890–1897.
34. Bull AMJ, Katchburian MV, Shih Y-F, Amis AA. Standardisation of the description of patellofemoral motion and comparison between different techniques. Knee Surg Sports Traumatol Arthrosc 2002;10: 184–193.
35. Powers CM, Ward SR, Fredericson M, Guillet M, Shellock FG. Patellofemoral kinematics during weight-bearing and non-weight-bearing knee extension in persons with lateral subluxation of the patella: a preliminary study. J Orthop Sports Phys Ther 2003;33:677–685.
36. McWalter EJ, Hunter DJ, Harvey WF, McCree P, Hirko KA, Felson DT, Wilson DR. The effect of a patellar brace on three-dimensional patellar kinematics in patients with lateral patellofemoral osteoarthritis. Osteoarthritis Cartilage 2011;19:801–808.
37. Draper CE, Besier TF, Santos JM, Jennings F, Fredericson M, Gold GE, Beaupre GS, Delp SL. Using real-time MRI to quantify altered joint kinematics in subjects with patellofemoral pain and to evaluate the effects of a patellar brace or sleeve on joint motion. J Orthop Res 2009;27:571–577.
38. Muhle C, Brinkmann G, Skaf A, Heller M, Resnick D. Effect of a patellar realignment brace on patients with patellar subluxation and dislocation: evaluation with kinematic magnetic resonance imaging. Am J Sports Med 1999;27:350–353.
39. Pfeiffer RP, DeBeliso M, Shea KG, Kelley L, Irmischer B, Harris C. Kinematic MRI assessment of McConnell taping before and after exercise. Am J Sports Med 2004;32:621–628.
40. Powers CM, Shellock FG, Beering TV, Garrido DE, Goldbach RM, Molnar T. Effect of bracing on patellar kinematics in patients with patellofemoral joint pain. Med Sci Sports Exerc 1999;31: 1714–1720.
41. Powers CM, Ward SR, Chan L-D, Chen Y-J, Terk MR. The effect of bracing on patella alignment and patellofemoral joint contact area. Med Sci Sports Exerc 2004;36:1226–1232.